Magnetochemical origin for Invar anomalies in iron-nickel alloys

V. Crisan,[1,*] P. Entel,[1,†] H. Ebert,[2,‡] H. Akai,[3,§] D. D. Johnson,[4,‖] and J. B. Staunton[5,¶]
[1]*Theoretical Physics, Gerhard-Mercator University, Lotharstraße 1, 47048 Duisburg, Germany*
[2]*Institute for Physical Chemistry, Ludwig-Maximilians University, Butenandtstraße 5-13, 81377 München, Germany*
[3]*Department of Physics, Osaka University, 1-1 Machikaneyama, Toyonaka, Osaka 560-0043, Japan*
[4]*Department of Materials Science and Engineering, University of Illinois, Urbana, Illinois 61801*
[5]*Department of Physics, University of Warwick, Coventry CV4 7AL, United Kingdom*
(Received 13 June 2001; revised manuscript received 14 January 2002; published 8 July 2002)

Zero- and finite-temperature (T) first-principles calculations versus composition (c) show that magnetochemical effects lead to Invar anomalies in Fe-(Ni, Co, Pt) alloys. Chemical short- or long-range order and negative interatomic exchange interaction of electrons in antibonding majority-spin states force the face-centered-cubic lattice to compete simultaneously for a smaller volume (from antiferromagnetic tendencies) and a larger volume (from Stoner ferromagnetic tendencies). The resulting additional negative lattice anharmonicity is very large for Fe-(Ni, Co) while absent for Fe-Pt. Our results explain the T- and c-dependent behavior of Invar properties, including the lattice softening and thermal expansion of Fe-Ni. In addition, the occurrence of a noncollinear spin structure at $T=0$ K near Invar can be understood on the basis of our results.

DOI: 10.1103/PhysRevB.66.014416 PACS number(s): 71.15.Nc, 81.30.Bx, 81.30.Kf, 64.75.+g

I. INTRODUCTION

Alloys of Fe and Ni have fascinated scientists for a century because of their intriguing properties: Chemical ordering (Ni rich), vanishing thermal expansion (Invar), and face-centered-cubic (fcc) to body-centered-cubic (bcc) structural transformations (Ni poor). Invar alloys are interesting because of their energetically quasidegenerate small-volume/low-moment (LM) and large-volume/high-moment (HM) ground states, thought to account for the extreme softness of the Fe-Ni lattice.[1] *Ab initio* calculations confirmed the existence of several energetically competing states[2–4] (and refs. therein) and showed that one can relate the Invar effect to the population of antibonding electronic states near the Fermi level E_F causing large internal pressure favoring a large volume and nonbonding states with lower internal pressure tending to a smaller volume.[2,4] However, this theoretical picture is unsatisfactory because it predicts a first-order HM-LM transition of the magnetic moments vs c in Fe-Ni, in contrast to experiment, and the softness of the fcc Fe-Ni alloys is not found.

Recent supercell calculations for $Fe_{66}Ni_{34}$ at $T=0$ K showed that noncollinear (NC) magnetism smears out the HM-LM transition giving rise to further negative lattice anharmonicity and a small bulk modulus B. As a consequence NC magnetism has been suggested to be the primary origin of the Invar effect,[5,6] even though temperature would destroy such a specific magnetic configuration. Calculations for ordered Fe_3Pt showed that NC magnetism is also important for Fe-Pt.[7] The origin of antiferromagnetic (AF) and NC order in the predominantly FM fcc Invar alloys can be traced back to an oscillatory exchange integral for fcc Fe,[8] where electrons in the antibonding majority-spin states below E_F prefer AF order,[9] which, however, cannot be realized because of natural frustration of the moments on the fcc lattice. Only AF or NC components are stable for sufficient chemical order which resembles elemental fcc Fe.

As a consequence the magnetic order in Invar alloys is very sensitive to small changes of the composition, the concentration fluctuations, the chemical order, and to the mutual interplay of all, various aspects of which were discussed (to name a few, further references can be found in the cited papers) in connection with experiment[10–22] and theory.[2–7,23–40]

In particular the calculations based on the Korringa-Kohn-Rostoker method within the coherent-potential-approximation (KKR-CPA) showed that chemical and magnetic disorder [represented by the disordered local-moment (DLM) theory[25,27,41]] leads to multiple competing magnetic states (even[42] in fcc Fe) and allows for additional lattice softening in the Fe-Ni alloys.[3] KKR-CPA-based thermodynamic linear-response calculations showed the importance of magnetocompositional interactions for the observed atomic-short-range order (ASRO) and $L1_2$ of FM permalloy, $FeNi_3$.[25,30] Here we address the pertinent question: Does chemical order extend to the Invar concentrations, and, if so, what role do the magneto-compositional effects in the Invar phenomenon play?

II. THEORETICAL APPROACH

In order to answer the question raised above, we have performed zero-temperature KKR calculations using a mul-

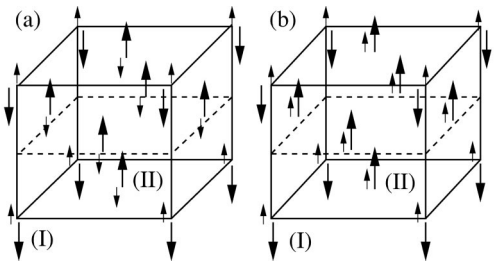

FIG. 1. Qualitative sketch of the magnetic order in Fe-Ni alloys as it results from the KKR-MS-CPA calculations for the two cases, increasing the local concentration of (a) Ni and (b) Fe on site II compared to site I by an amount S. Large arrows: Fe moments, small arrows: Ni moments.

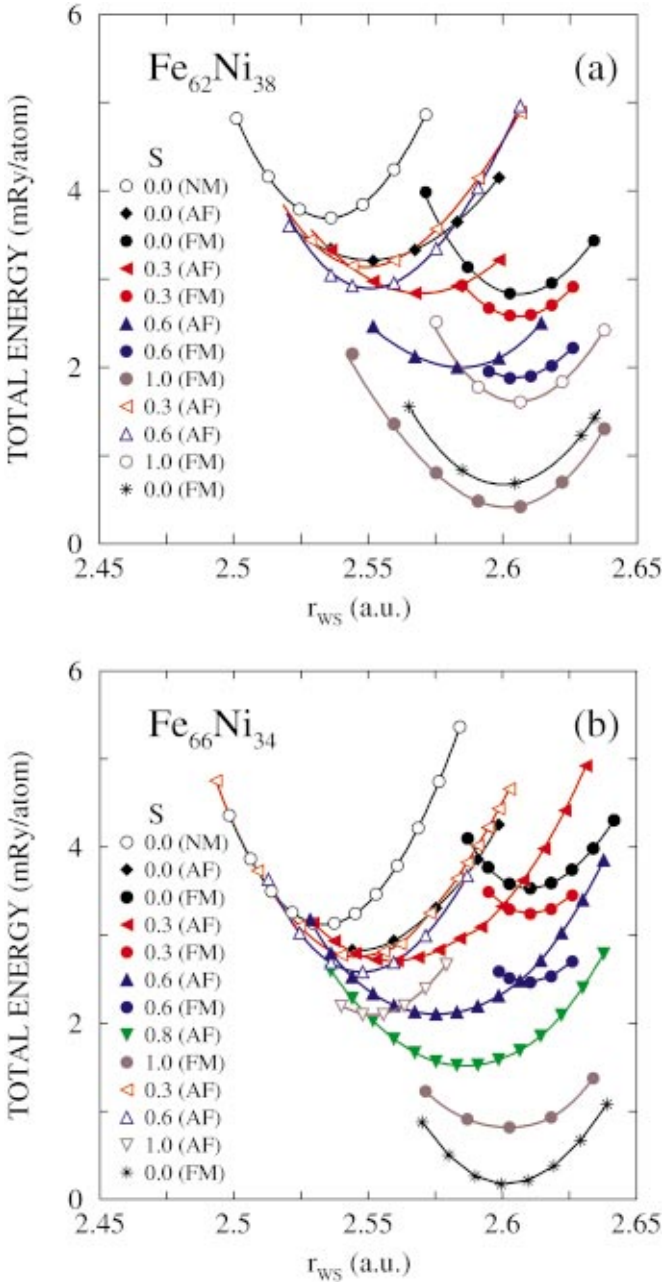

FIG. 2. (Color) Total energy per atom of (a) $Fe_{62}Ni_{38}$ and (b) $Fe_{66}Ni_{34}$ (relative to some arbitrary energy zero) as a function of the Wigner-Seitz radius for different values of S. Apart from the NM $S=0$ solution the open symbols refer to case (a) and the full symbols to case (b), see text for explanation. Stars refer to the bcc phase. For all figures, ''AF'' refers to any admixture of AF components.

tisublattice extension of the CPA (KKR-MS-CPA),[43,44] while calculations for $T\neq 0$ make use of the inhomogeneous version of the single-site CPA and an electronic theory of ASRO.[45]

The KKR-MS-CPA allows for inequivalent atoms in the unit cell with different local site concentrations of the constituents.[43,44] Two cases are considered over the whole concentration range of $Fe_{c_{Fe}}Ni_{c_{Ni}}$: In case (a) [(b)] we reduce the local concentration of Ni [Fe] by an amount S [a long-range-order (LRO) parameter] at the corner site (I) and add it to the face-centered site (II),

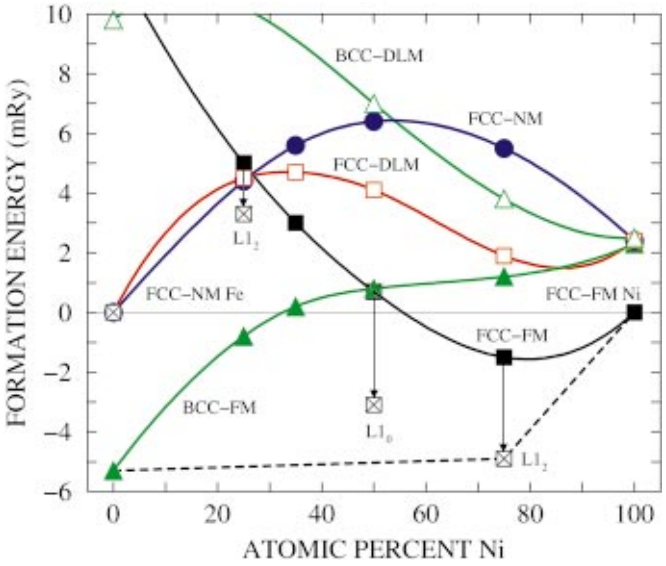

FIG. 3. (Color) ΔE_f (mRy) versus percent Ni, the formation energy per atom (relative to fcc NM Fe and FM Ni) for various magnetic and chemical states: Filled circles = NM; squares filled = FM, open = DLM, crossed = ordered; triangles filled = bcc FM, open = bcc DLM. Arrows connect the disordered to fully ordered FM $L1_2$ and $L1_0$ states. The dashed line represents the $T=0$ K Maxwell construction of lowest energy states: bcc FM Fe, $L1_2$ FM Ni_3Fe, and fcc FM Ni.

$$\text{Case (a):}\quad c^{\mathrm{I}}_{\mathrm{Ni}}=[1-S(a)]c_{\mathrm{Ni}},\quad c^{\mathrm{I}}_{\mathrm{Fe}}=1-c^{\mathrm{I}}_{\mathrm{Ni}},$$

$$c^{\mathrm{II}}_{\mathrm{Ni}}=[1+\tfrac{1}{3}S(a)]c_{\mathrm{Ni}},\quad c^{\mathrm{II}}_{\mathrm{Fe}}=1-c^{\mathrm{II}}_{\mathrm{Ni}},$$

$$\text{Case (b):}\quad c^{\mathrm{I}}_{\mathrm{Fe}}=[1-S(b)]c_{\mathrm{Fe}},\quad c^{\mathrm{I}}_{\mathrm{Ni}}=1-c^{\mathrm{I}}_{\mathrm{Fe}},$$

$$c^{\mathrm{II}}_{\mathrm{Fe}}=[1+\tfrac{1}{3}S(b)]c_{\mathrm{Fe}},\quad c^{\mathrm{II}}_{\mathrm{Ni}}=1-c^{\mathrm{II}}_{\mathrm{Fe}}. \qquad (1)$$

The resulting magnetic ordering tendencies for cases (a) and (b) for the Fe-rich alloys are sketched in Fig. 5. For $S(a)=1$ or $S(b)=1$, Ni or Fe is completely removed from site I [if the index (a) or (b) is omitted for S in the following, it applies to both cases]. Thus, we represent the increase of LRO by a continuous progression from a homogeneously disordered state ($S=0$) to maximal order ($S=1$) (Fig. 1).

It should be stressed that the partial LRO for the KKR-MS-CPA calculations is related to the pair correlations and atomic short-range order, as detailed recently in the system Ni_3V.[44] The total energy data from these calculations for $T=0$ K will be used below to investigate Invar anomalies—in particular the thermal expansion—at finite temperatures. To allow for a more direct connection of electronic structure data and finite temperature properties, a KKR-CPA based linear-response formalism is used that explicitly accounts for ASRO at finite temperature. The key results obtained via ASRO calculations are consistent with those obtained via partial chemical LRO at $T=0$ K using the KKR-MS-CPA.

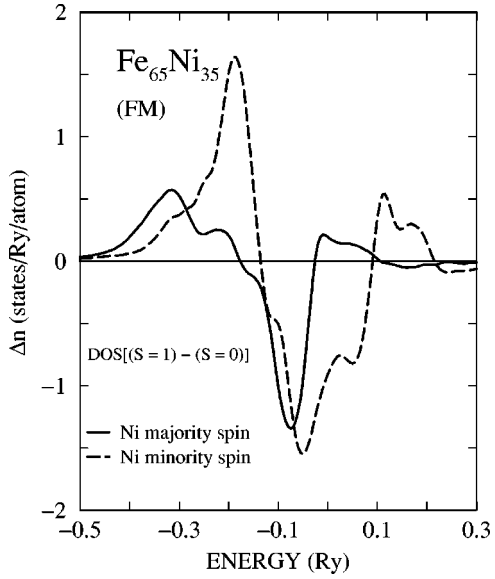

FIG. 4. Difference of density of states of Ni per unit cell between the fully ordered ($S=1$) and completely disordered ($S=0$) phases for $Fe_{65}Ni_{35}$. The corresponding difference for Fe (not shown here) is smaller.

The KKR-MS-CPA calculations (local spin density with Moruzzi-Janak-Williams parametrization[46]) have been carried out for fcc and bcc Fe-Ni alloys with various compositions, $Fe_{64.2}Ni_{31.0}Co_{4.8}$ (super Invar) and $Fe_{72}Pt_{28}$ for $0 \leqslant S \leqslant 1$ using 35 k points in the irreducible Brillouin zone, maximum angular momentum $l_{max}=3$, and an accuracy of 10^{-4} mRy for the total energy. For comparison of multiple disordered states, the formation energy ΔE_f vs c was obtained with 120 k points and $l_{max}=2$, using the atomic sphere approximation.

III. RESULTS AND DISCUSSION

We find that maximal order ($S=1$) leads to the lowest energy for all alloys considered here, see, e.g., Fig. 2. But there is a marked difference between Ni- and Fe-rich alloys. For Ni-rich alloys it is more favorable to move Ni from site I to II, case (a), whereas the energy is lower when moving Fe from I to II, case (b), for Fe-rich alloys (curves with full symbols in Fig. 2). The equilibrium phase diagram of Fe-Ni shows that ordering in the fcc structure occurs on the Ni-rich side and that otherwise the alloys decompose into $FeNi_3$ and bcc Fe.[47] Our ΔE_f vs c results for NM, FM, DLM chemically disordered fcc and bcc alloys, and chemically ordered FM fcc alloys (Fig. 3) clearly indicate the low-T equilibrium should be phase segregated into FM bcc Fe and $L1_2$ $FeNi_3$. NM means that there are no moments on the site, i.e., a nonmagnetic state in the parlance of Stoner theory; the other nonmagnetic state is the DLM with random orientations of the moments so that the thermal average above T_c gives zero magnetization. However, one must note that the experimentally as-prepared Fe-Ni samples are not in equilibrium. Therefore, the nonequilibrium fcc-based results are directly relevant to the measured ones. The important consequence is that it is the nonequilibrium (local) chemical order in the fcc cases that gives rise to the Invar anomaly.

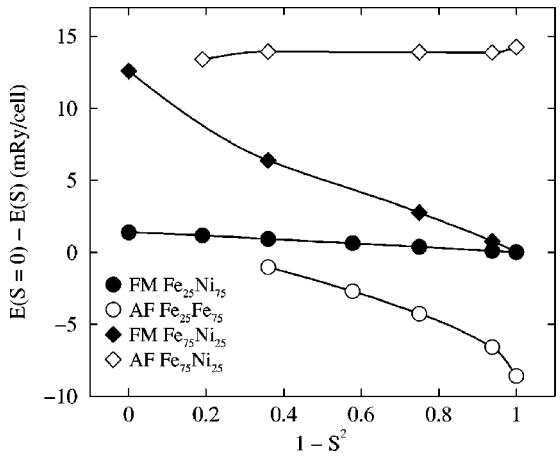

FIG. 5. $E(S=0)-E(S)$ versus $1-S^2$ for $L1_2$-based ordering in $Fe_{25}Ni_{75}$ and $Fe_{75}Ni_{25}$. The $S=0$ FM solution for a given c_{Ni} was used as reference state; as before "AF" refers to any admixture of FM and AF components. Positive y axis indicates most stable state. See text for discussion.

Figure 2 shows the total energies for $Fe_{62}Ni_{38}$ and $Fe_{66}Ni_{34}$ as a function of the Wigner-Seitz radius r_{WS}, where $(4\pi/3)r_{WS}^3$ is the atomic volume. For the disordered state $S=0$ of $Fe_{62}Ni_{38}$, the nonmagnetic (NM) and FM states lie close in energy, with the FM state the lower one. The situation is similar for $Fe_{72}Pt_{28}$ (not shown here). High-T Fe-Ni samples have average magnetic moments of $1.42\mu_B$/atom; thus, although close in energy, the NM state is not relevant, whereas the paramagnetic DLM is, as Fig. 3 shows. DLM also gives the correct high-T moments.[3] The curves show that when approaching the paramagnetic (DLM) high-temperature phase, the two minima of the fcc-FM and the fcc-DLM curves would have to reverse their order, leading in between to low thermal expansion. For $Fe_{66}Ni_{34}$ being outside the Invar concentration range by just 1 at %, the situation is different since now the NM and AF states are lower in energy.

However, for $S \neq 0$ the situation changes completely and illustrates the different behavior of Fe-Ni and Fe-Pt alloys. First, the total energy decreases with increasing S for all Invar alloys (see discussions for Figs. 2–4). Second, the curvature of the total energy, which is proportional to the bulk modulus, becomes much smaller in case of Fe-Ni, whereas the lattice of Fe-Pt alloys hardens upon ordering (see discussion for Fig. 6). Furthermore, the partial order in the Fe-Ni alloys causes the energy barrier, which exists for $S=0$ between the LM (i.e., the DLM) and HM states, to vanish for finite S. Softening of similar extent was also observed in Ref. 6 in calculations for NC moments.

But there are important differences with respect to the work in Ref. 6, for we find in case of Fe-Ni Invar alloys, regardless of the value of S, two sets of competing FM HM high-volume and LM low-volume solutions, where the LM low-volume solutions exhibit large AF components in the predominantly FM alloys which are induced by the partial chemical order in the alloys (AF in Fig. 2 indicates parallel and antiparallel moments on sites II and I, respectively, see Fig. 1). For $Fe_{62}Ni_{38}$ the FM HM solutions are lower in

TABLE I. Chemical and magnetic trends in fcc $Fe_{1-c}Ni_c$. Here a is the equilibrium lattice constant, FM and DLM refer to ferromagnetic and paramagnetic states, $\mathbf{q}$ is the wave vector (in units of $2\pi/a$) for which $S^{(2)}(\mathbf{q})$ has a maximum, and the atom pair-correlation function diverges at the spinodal (see text) T_s. The total energy is in Ry/atom and shows the relative stability of the FM and DLM phases. At $S\neq 0$ for $c=0.25$, $L1_2$ with AF components is lower (see text) than both FM and DLM below the magnetic transition.

c	a (a.u.)	State	$\mathbf{q}$	T_s (K)	Energy (Ry)	Tendency
0.25	6.716	FM	(0,0,1)	450	-2645.0283	$L1_2$/FM
0.25	6.600	DLM	(0,0,0)	665	-2645.0287	Clustering/AF
0.35	6.700	FM	(0,0,1)	590	-2693.9123	$L1_2$/FM
0.35	6.600	DLM	(0,0,0)	700	-2693.9106	Clustering/AF
0.50	6.650	FM	(0,0,1)	670	-2767.2378	$L1_0$/FM
0.50	6.650	DLM	$(0,\frac{1}{2},1)$	<100	-2767.2344	$D0_{22}$/AF
0.75	6.650	FM	(0,0,1)	240	-2889.4487	$L1_2$/FM
0.75	6.650	DLM	$(0,\frac{1}{2},1)$	<200	-2889.4419	$D0_{22}$/AF

energy confirming the experimental observation that Invar alloys are predominantly magnets with large ferromagnetic moments,[40,48] although the energetic difference to the AF solutions is small. With increasing iron content the AF solutions become lower in energy, see Fig. 2(b), showing that there is a smooth crossover from FM HM to LM (AF) states in the Fe-Ni Invar alloys. In addition, we have the DLM states (which are high-T NC states) which compete in energy. The change of the total-energy curves with S in the case of super-Invar $Fe_{64.2}Ni_{31.0}Co_{4.8}$ is similar to the case $Fe_{62}Ni_{38}$. There is no breakdown of the magnetic moment in fcc Fe-Ni for $x\lesssim 35$. But the calculations show a crossover from fcc to bcc right at $x=35$ at % Ni in perfect agreement with experiment, see Figs. 2 and 3.

The origin of the decrease in ground-state energy with increasing chemical order can be ascribed to an increase of the Madelung energy contribution to the total energy. On the other hand an important change is seen in the partial density of states of Fe and Ni upon chemical ordering. The corresponding result for Ni, $\Delta n_{\mathrm{Ni}}=n_{\mathrm{Ni}}(S=1)-n_{\mathrm{Ni}}(S=0)$ (where n is the density of states in Fig. 4), shows that partial order leads for both spin channels to a downward shift of the density of states, thus lowering the energy. With increasing $S(b)$ (when moving Fe by an amount S from site I to II) the maximum of the probability distribution function (not shown here) of finding a certain number of Fe nearest-neighbor (NN) atoms around site I is increasing from its average value of 7.8 NN (0.65×12) for $S=0$ to ≈ 11 NN for S values close to 1 (with a single Ni atom on site I) which favors the corresponding tiny Ni charge transfer (in the inhomogeneous CPA) as well as the AF ordering tendency due to the similarity of the alloy for $S=1$ to elemental fcc Fe.

The importance of the local chemical environment for ordering in alloys and its influence on the electronic structure and charge densities, which is the basis of the theory of ordering using the inhomogeneous CPA, is discussed in Ref. 49. The connection of ASRO measurements (or calculations) to LRO calculations (i.e., $S>0$), including the important effects due to LRO configurational excitations, was discussed in Ref. 44, where, in addition, the applicability of LRO calculations to states with ASRO was made via a second-order expansion of $E(S)$. Following Ref. 44, if $E(S=0)-E(S)$ scales linearly in S^2, then the ordering energetics, as well as the electronic structure and magnetic states, are dominated by pairwise correlations (which, for small S, are directly related to the ASRO,[44] whereas deviations from S^2 indicate important correlations beyond pairwise).

In Fig. 5, we have plotted $E(S=0)-E(S)$ versus $1-S^2$ for $L1_2$-type ordering in $Fe_{25}Ni_{75}$ and $Fe_{75}Ni_{25}$ for FM and AF states. In agreement with finite-T ASRO calculations discussed below, a tendency for $L1_2$ ordering in the Fe-Ni alloys is found for the low-energy structures with FM (AF) solution in the Ni-rich (Ni-poor) regions. The ordering energy of FM $Fe_{25}Ni_{75}$ exhibits linear behavior for all S, whereas AF $Fe_{75}Ni_{25}$ is linear from $S=0.3-0.8$. (The linear regime for $S\approx 0$ is appropriate to high-T equilibrium state and indicates an initial stronger local tendency to $L1_2$ order). Hence, we expect the experimental results from nonequilibrium samples near $c_{Ni}\approx 0.25$ should be compared to calculated results from $S=0.3-0.8$.

We will use the $S=0.3-0.8$ states of AF $Fe_{65}Ni_{35}$ and $Fe_{66}Ni_{34}$ for direct calculation of the lattice softening (B and B') and linear thermal expansion, $\alpha(T)$. First, however, we explicitly study the high-T ASRO, and verify our results for weak partially LRO states, by direct calculation of the Warren-Cowley pair correlations in a binary solid solution, as defined by

$$\alpha_{ij}=\frac{\langle\xi_i\xi_j\rangle-\langle\xi_i\rangle\langle\xi_j\rangle}{k_BTc(1-c)} \tag{2}$$

with lattice Fourier transform

$$\alpha(\mathbf{q};T)=[k_BT-c(1-c)S^{(2)}(\mathbf{q};T)]^{-1}. \tag{3}$$

Here ξ_i is the occupation variable of site $\mathbf{R}_i$ with concentration $c=\langle\xi_i\rangle$, and $S^{(2)}$ is related to the second derivative with respect to the concentration of the electronic grand potential,[45] evaluated here within the KKR-CPA. The wave-vector $\mathbf{q}_{max}$ where $S^{(2)}(\mathbf{q})$ and therefore $\alpha(\mathbf{q})$ are maximal indicates the ordering periodicity the ASRO would tend below a phase boundary, and appropriate for kinetically limited

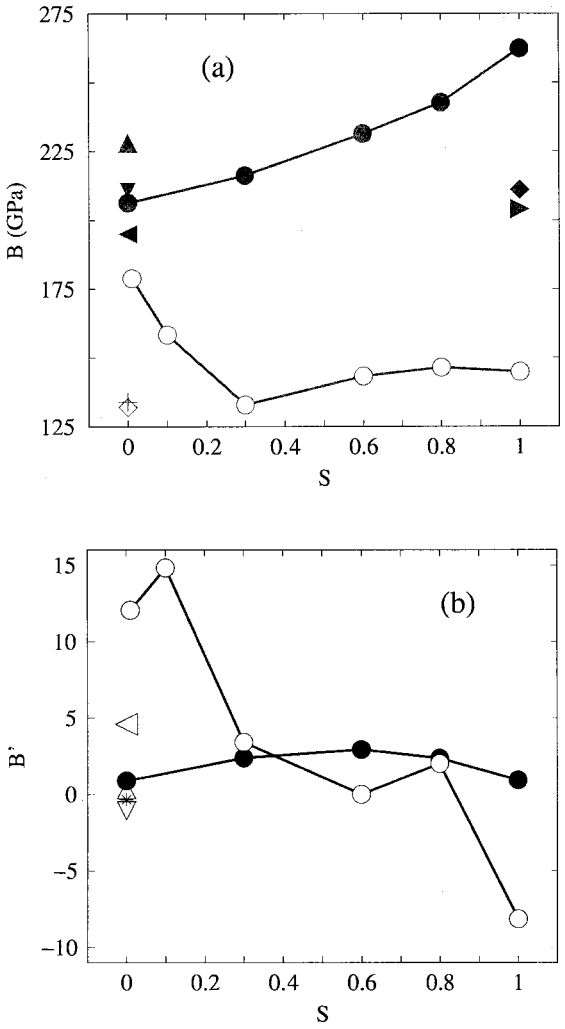

FIG. 6. Calculated bulk modulus (a) and its pressure derivative (b) of $Fe_{66}Ni_{34}$ (open circles) and $Fe_{72}Pt_{28}$ (filled circles) compared to experimental and other theoretical data (B, $S=0$): Open diamond and plus sign for $Fe_{64}Ni_{36}$ (Ref. 52) and $Fe_{64.7}Ni_{35.3}$; filled (Ref. 53) triangle down, up and left (Ref. 54) for $Fe_{75}Pt_{25}$, $Fe_{70}Pt_{30}$, and $Fe_{72}Pt_{28}$ (Refs. 34 and 57), respectively. $S=1$: Filled-triangle right and diamond for Fe_3Pt (Ref. 55) at constant magnetic field and constant magnetization, respectively. Experiment (B', $S=0$): Open triangle down and star for $Fe_{58}Ni_{42}$ and $Fe_{64}Ni_{36}$ (Ref. 52); open triangles left and up (Ref. 56) for $Fe_{64.7}Ni_{35.3}$ and $Fe_{65}Ni_{35}$, respectively (Ref. 58).

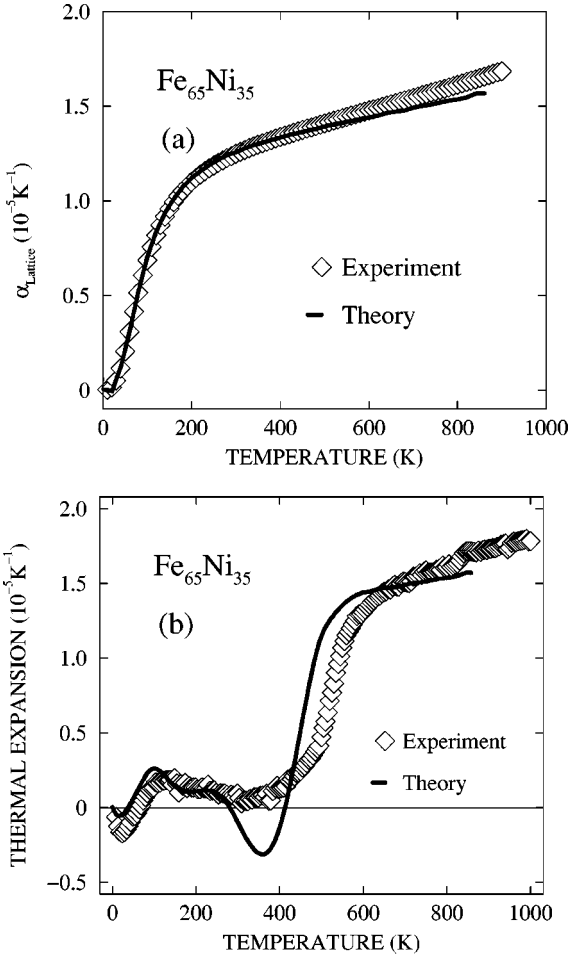

FIG. 7. Thermal-expansion coefficient of $Fe_{65}Ni_{35}$ as a function of temperature, (a) the lattice contribution with the magnetic part subtracted, and (b) the total contribution.

or quenched samples. The maximal instability to ordering is given when $\alpha(\mathbf{q};T)$ diverges which defines the spinodal temperature, $T_s=c(1-c)S^{(2)}(\mathbf{q}_{max})/k_B$. Similar to the chemical susceptibility $\alpha(\mathbf{q})$ based on the inhomogeneous CPA, we also calculate the paramagnetic susceptibility $\chi(\mathbf{q};T)$ via the formalism of Ref. 30 that uses the DLM paramagnetic state as an (approximate) reference state.

Finite-T ordering tendency and estimate T_s for Fe-Ni in FM and DLM states are listed in Table I. The results essentially confirm the zero-temperature findings of chemical and AF ordering tendencies in Fe-rich alloys. Throughout the whole concentration range FM order for $S=0$ state is shown to promote chemical order characterized by a (0,0,1) concentration wave, i.e., $L1_0$ or $L1_2$ ordering. In the DLM states of the Fe-rich alloys, chemical clustering is encouraged alongside the growth of weak incommensurate AF magnetic correlations. However, as the Ni content is increased these correlations become FM and the chemical clustering tendencies disappear in favor of weak ordering, e.g., $Fe_{25}Ni_{75}$ in Table I.

For FM $Fe_{50}Ni_{50}$ $S^{(2)}(\mathbf{q})$ has a maximum at (0,0,1) and a transition temperature T_s of 670 K into an $L1_0$ state but the total-energy calculations reveal that this is a local minimum and the observed phase segregated bcc Fe and $L1_2$ $FeNi_3$ is the most stable, see Fig. 3.

In $Fe_{75}Ni_{25}$ the DLM state is slightly lower in energy than the FM state and, from $\chi(\mathbf{q})$, we find weak incommensurate AF correlations between the local moments on the iron atoms. For $Fe_{65}Ni_{35}$ the DLM state is just above the FM state in energy and there remain weak AF correlations between the Fe local moments. The magnetic correlations peak at $\mathbf{q}=(0,0,0.6)$ with significant weight also around $\mathbf{q}=(0,0.6,0.6)$. Indeed neutron data show peaks near $\mathbf{q}\approx(0,0.5,0.5)$. The Fermi surface of DLM $Fe_{66}Ni_{34}$ estimated from the spectral function $S(\mathbf{q},\varepsilon_F)$ shows nesting for this particular $\mathbf{q}$ vector in the absence of chemical order ($S=0$)

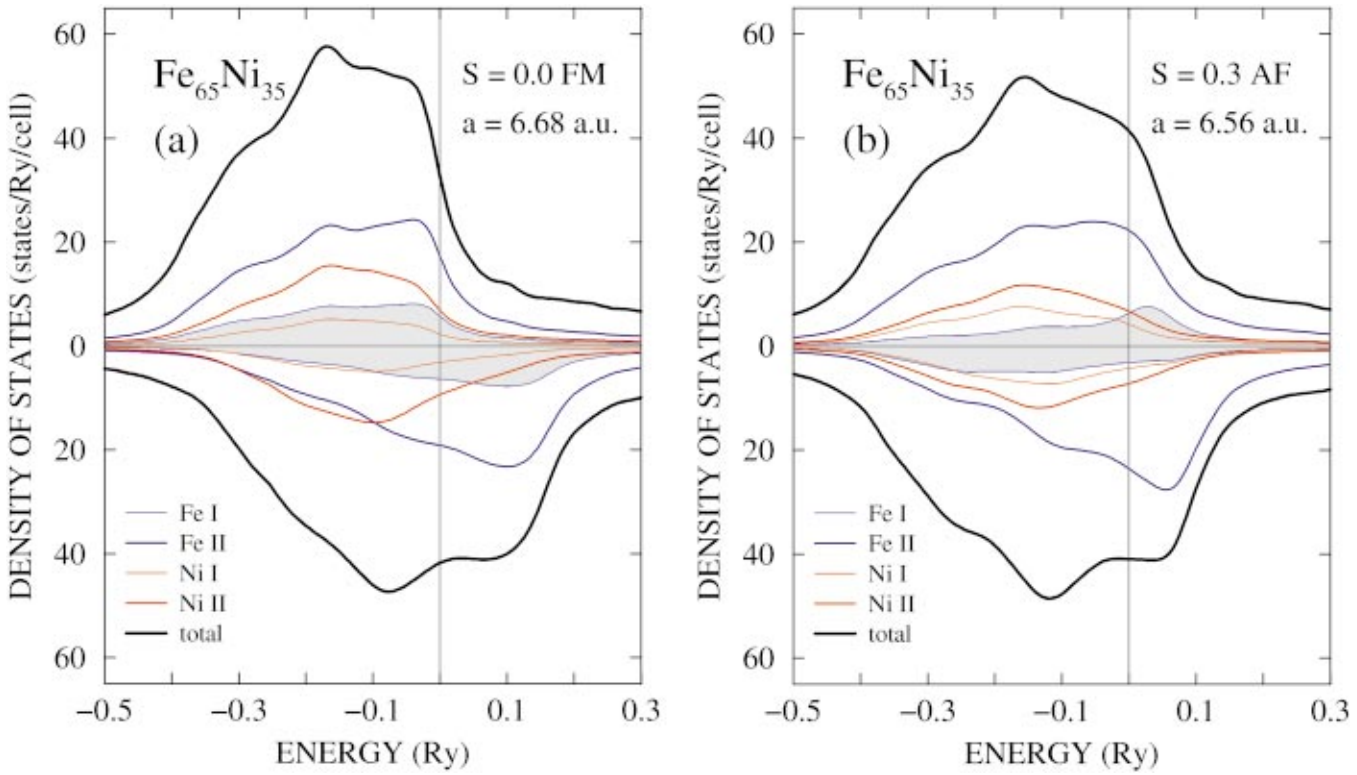

FIG. 8. (Color) (a) Density of states of ferromagnetic $Fe_{65}Ni_{35}$ with no local chemical order ($S=0$) and (b) of ferromagnetic $Fe_{65}Ni_{35}$ with antiferromagnetic components induced by chemical order ($S=0.3$).

as well as nesting for smaller **q** vectors. The nesting considerably increases when allowing for chemical order ($S=0.3$) and AF components. For both of these alloys in their paramagnetic states there are chemical clustering correlations, in sharp distinction to those prevalent in the FM counterparts. Hence chemical ordering and clustering directly compete, but, as show Figs. 2, 3, and 5, $L1_2$ is favored but with a crossover from FM to AF near Invar.

Figure 6 shows the bulk modulus B and its pressure derivative B' for $Fe_{66}Ni_{34}$ and $Fe_{72}Pt_{28}$. With increasing S, B decreases for Fe-Ni, thereby approaching the experimental values, while there is a systematic increase of B for Fe-Pt. The lowest value of B for Fe-Ni being closest to the experimental value corresponds to $S=0.3$, which is weak LRO and reflects also ASRO (as discussed above). Experimental values for B' are around zero in the case of Fe-Ni; calculated values are found to be small for $0.3 \leqslant S \leqslant 0.8$. Thus, the agreement between our first-principles results and experiment for B and B' is satisfying and the first agreement of this kind.

In order to get further feeling for the additional softness of the lattice for finite S in case (b), we have calculated the thermal-expansion coefficient for $Fe_{65}Ni_{35}$ with $S=0.3$, see Fig. 6. We chose $S=0.3$ because it is in the intial range of S values for which the bulk modulus is small. For $S=0.3$ the energetically most favorable state consists of FM aligned spins on sites II and an AF component on site I. We denote its corresponding energy by $E_{0.3}$. The final paramagnetic state (for $S=0.3$) was chosen to have zero magnetic moment on site I and spin-up and spin-down components of equal magnitude on site II so that the average magnetic moment per cell is zero (corresponding essentially to a DLM state with energy $E_{0.3}^{\mathrm{DLM}}$). The calculated total-energy curve that passes through $E_{0.3}$ and $E_{0.3}^{\mathrm{DLM}}$ is then used for the evaluation of the magnetic contribution to the thermal-expansion coefficient. This is essential since the decrease in volume when passing from the $E_{0.3}$ to $E_{0.3}^{\mathrm{DLM}}$ states is much smaller compared to the case when choosing the NM state as high-temperature reference state. The thermal-expansion coefficient was then evaluated in two steps. First, we evaluated the nonmagnetic lattice contribution by making use of the Debye-Grüneisen model (see Refs. 36 and 50 for details), whereby the magnetic contribution (~ 6) had to be subtracted from the Grüneisen γ, $\gamma \sim \frac{1}{2}(1+B')$, yielding $\alpha_{\mathrm{Lattice}}$ shown in Fig. 7(a) which agrees with the experimental result apart from a small deviation at high temperatures (the experimental procedure of decomposing α is discussed in Ref. 19). In order to obtain $\alpha_{\mathrm{Magnetic}}$ we use the experimental $M(T)/M(O)$ as[51] input. For a given temperature T we compare this magnetization with the corresponding value of the $E_{0.3}$–$E_{0.3}^{\mathrm{DLM}}$ curve. This leads to a hypothetical temperature dependent $V(T)$ curve yielding the corresponding $\alpha_{\mathrm{Magnetic}}$ contribution. The sum of both contributions to the thermal-expansion coefficient is shown in Fig. 7(b) being in rather satisfying agreement with the experimental data. However we note that this procedure will lead to similar results for $\alpha(T)$ for other S values, provided that the tendency for an admixture of AF components to the FM alloy is taken into account and the correct DLM state is chosen.

IV. SUMMARY AND CONCLUSIONS

To summarize we have shown that (local) chemical order and magnetochemical coupling are of central importance for the Invar alloys. It leads to metastable states, competing FM and AF order, and additional lattice softening for the Fe-Ni alloys at low temperatures in agreement with experiment. The results highlight that temperature- and composition-dependent Invar effects require more than solely noncollinear spin arrangements to explain lattice softening. The zero-temperature FM solutions are lower in energy in the Invar region showing the Invar state is predominantly a HM high-volume state. However, when approaching the critical composition $Fe_{65}Ni_{35}$ the competing AF solutions (FM solutions with AF components) supported by local chemical order, gradually become lower in energy than the FM HM high-volume solutions. Finite-T calculations of the atomic pair correlations underline the observed chemical trends for ordering and AF correlations for Fe-rich alloys that we found for partially LRO states.

Further intriguing characteristics related to Invar and martensitic behavior of the Fe-Ni alloys such as the different populations of e_g and t_{2g} orbitals proposed earlier[4] have recently been discussed and questioned on the basis of polarized neutron scattering on $Fe_{65}Ni_{35}$.[48] But these experiments show changes of the population when the external magnetic field is changed from 4.6 T to 9.0 T, where the higher field forces the magnetic moments of Fe to reach their saturation value of $\sim 2.86\ \mu_B$ on the fcc lattice. Smaller changes can probably not be resolved by experiment, which should be extended to other compositions as well. The suggestion in Ref. 48 to consider the (dynamic) implications of instabilities in the band structure has been accounted for in this paper by calculating over the whole concentration range the divergence of the atomic pair-correlation function and magnetic susceptibilities, as well as formation energetics, which reproduce general trends from spinodal ordering in the Ni-rich region to segregation or clustering in the Fe-rich part of the phase diagram. The development of AF tendencies around the critical Invar concentration of 65 at % Fe might have been suppressed by the large external magnetic field in the recent neutron scattering experiment. As discussed above, there are other experimental hints coming, for example, from hyperfine-field measurements which point towards AF (spin canting) contributions.[16] The amount of change in the occupation of t_{2g} states (practically no change of occupation of e_g orbitals) going hand in hand with admixture of AF components for $S=0.3$ in the predominantly FM $Fe_{65}Ni_{35}$ can be estimated from Fig. 8.

Other intriguing Invar properties such as the anomalous behavior of the hyperfine field under pressure[59] or the forbidden (spin phonon?) excitations observed in neutron-scattering experiments[60] require further exploration.

ACKNOWLEDGMENTS

P.E. would like to thank Eberhard Wassermann for continued interest and helpful discussions and Mehmet Acet for providing us with the lattice thermal-expansion data of Fe-Ni alloys extracted from the experiment. D.D.J. is funded by the Department of Energy at the Frederick Seitz Materials Research Laboratory (Contract No. DEFG02-ER964539).

*Permanent address: Department of Physics, Babes-Bolyai University, Kogalniceanu 1, 3400 Cluj-Napoca, Romania. Email address: crisan@thp.uni-duisburg.de

†Email address: entel@thp.uni-duisburg.de

‡Email address: hubert.ebert@cup.uni-muenchen.de

§Email address: akai@phys.sci.u-osaka.ac.jp

‖Email address: duanej@uiuc.edu

¶Email address: j.b.staunton@warwick.ac.uk

[1] R. J. Weiss, Proc. Phys. Soc. London **82**, 281 (1963).

[2] J. Kaspar and D. R. Salahub, Phys. Rev. Lett. **47**, 54 (1981).

[3] D. D. Johnson, F. J. Pinski, J. B. Staunton, B. L. Gyorffy, and G. M. Stocks, in *Physical Metallurgy of Controlled Expansion Invar-Type Alloys*, edited by K. C. Russell and D. F. Smith (TMS, Warrendale, PA, 1990), p. 3; D. D. Johnson and W. A. Shelton, in *The Invar Effect: A Centennial Symposium*, edited by J. Wittenauer (TMS, Warrendale, PA, 1997), p. 63.

[4] P. Entel, E. Hoffmann, P. Mohn, K. Schwarz, and V. L. Moruzzi, Phys. Rev. B **47**, 8706 (1993).

[5] Y. Wang, G. M. Stocks, D. M. C. Nicholson, and W. A. Shelton, J. Appl. Phys. **81**, 3873 (1997).

[6] M. van Schilfgaarde, I. A. Abrikosov, and B. Johansson, Nature (London) **400**, 46 (1999).

[7] M. Uhl, L. M. Sandratskii, and J. Kübler, Phys. Rev. B **50**, 291 (1994).

[8] Y.-M. Zhou, D.-S. Wang, and Y. Kawazoe, Phys. Rev. B **59**, 8387 (1999).

[9] R. F. Sabiryanov, S. K. Bose, and O. N. Mryasov, Phys. Rev. B **51**, 8958 (1995).

[10] S. F. Dubinin, S. K. Sidorov, S. G. Teploukhov, and V. E. Arkhipov, Zh. Eksp. Teor. Fiz., Pis'ma Red. **18**, 550 (1973) [JETP Lett. **18**, 324 (1974)].

[11] J. F. Petersen, M. Aydin, and J. M. Knudsen, Phys. Lett. **62A**, 192 (1977).

[12] H. Zähres, M. Acet, W. Stamm, and E. F. Wassermann, J. Magn. Magn. Mater. **72**, 80 (1988).

[13] D. G. Rancourt, S. Chehab, and G. Lamarche, J. Magn. Magn. Mater. **78**, 129 (1989).

[14] E. F. Wassermann, in *Ferromagnetic Materials*, edited by K. H. J. Buschow and E. P. Wohlfarth (North-Holland, Amsterdam, 1990), p. 240.

[15] A. Wiedemann, Q. Li, W. Wagner, and W. Petry, Physica B **180&181**, 793 (1992).

[16] J. Y. Ping, D. G. Rancourt, and R. A. Dunlap, J. Magn. Magn. Mater. **103**, 285 (1992).

[17] G. Dumpich, J. Kästner, U. Kirschbaum, H. Mühlbauer, J. Liang, Th. Lübeck, and E. F. Wassermann, Phys. Rev. B **46**, 9258 (1992).

[18] D. G. Rancourt and R. B. Scorzelli, J. Magn. Magn. Mater. **150**, 30 (1995).

[19] T. Schneider, M. Acet, B. Rellinghaus, E. F. Wassermann, and W. Pepperhoff, Phys. Rev. B **51**, 8917 (1995).

[20] J. L. Robertson, G. E. Ice, C. J. Sparks, X. Jiang, P. Zschack, F.

Bley, S. Lefebvre, and M. Bessiere, Phys. Rev. Lett. **82**, 2911 (1999).
[21] E. F. Wassermann, M. Acet, P. Entel, and W. Pepperhoff, Magn. Soc. Jpn. **23**, 385 (1999).
[22] D. G. Rancourt, K. Lagarec, A. Densmore, and R. A. Dunlap, J. Magn. Magn. Mater. **191**, L255 (1999).
[23] H. Hasegawa and J. Kanamori, J. Phys. Soc. Jpn. **31**, 382 (1971); **33**, 1599 (1971).
[24] A. R. Williams, V. L. Moruzzi, C. D. Gelatt, Jr., and J. Kübler, J. Magn. Magn. Mater. **31-33**, 88 (1983).
[25] J. B. Staunton, D. D. Johnson, and B. L. Gyorffy, J. Appl. Phys. **61**, 3693 (1987).
[26] Y. Kakehashi, Physica B **161**, 143 (1989).
[27] J. B. Staunton and B. L. Gyorffy, Phys. Rev. Lett. **69**, 371 (1992).
[28] H. Akai and P. H. Dederichs, Phys. Rev. B **47**, 8739 (1993).
[29] J. B. Staunton, Rep. Prog. Phys. **57**, 1289 (1994).
[30] M. F. Ling, J. B. Staunton, and D. D. Johnson, J. Phys.: Condens. Matter **6**, 5981 (1994).
[31] I. A. Abrikosov, O. Eriksson, P. Söderlind, H. L. Skriver, and B. Johansson, Phys. Rev. B **51**, 1058 (1995).
[32] M. Schröter, H. Ebert, H. Akai, P. Entel, E. Hoffmann, and G. G. Reddy, Phys. Rev. B **52**, 188 (1995).
[33] M. Z. Dang and D. G. Rancourt, Phys. Rev. B **53**, 2291 (1996).
[34] R. Hayn and V. Drchal, Phys. Rev. B **58**, 4341 (1998).
[35] P. James, O. Eriksson, B. Johansson, and I. A. Abrikosov, Phys. Rev. B **59**, 419 (1999).
[36] H. C. Herper, E. Hoffmann, and P. Entel, Phys. Rev. B **60**, 3839 (1999).
[37] K. Lagarec and D. G. Rancourt, Phys. Rev. B **62**, 978 (2000).
[38] P. Entel, H. C. Herper, E. Hoffmann, G. Nepecks, E. F. Wassermann, M. Acet, V. Crisan, and H. Akai, Philos. Mag. B **80**, 141 (2000).
[39] P. Entel, E. Hoffmann, H. C. Herper, E. F. Wassermann, V. Crisan, H. Ebert, and H. Akai, J. Phys. Soc. Jpn. **69**, 112 (2000).
[40] D. G. Rancourt, Phase Transit. **75**, 201 (2002).
[41] B. L. Gyorffy, A. J. Pindor, J. B. Staunton, G. M. Stocks, and H. Winter, J. Phys. F: Met. Phys. **15**, 1387 (1985).
[42] F. J. Pinski, J. Staunton, B. L. Gyorffy, D. D. Johnson, and G. M. Stocks, Phys. Rev. Lett. **56**, 2096 (1986).
[43] H. Akai, Phys. Rev. Lett. **81**, 3002 (1998).
[44] D. D. Johnson, A. V. Smirnov, J. B. Staunton, F. J. Pinski, and W. A. Shelton, Phys. Rev. B **62**, R11 917 (2000).
[45] B. L. Gyorffy and G. M. Stocks, Phys. Rev. Lett. **50**, 374 (1983).
[46] V. L. Moruzzi, J. F. Janak, and A. R. Williams, *Calculated Electronic Properties of Metals* (Pergamon, New York, 1978).
[47] O. Kubaschewski, *Iron - Binary Phase Diagrams* (Springer, Berlin, 1982), p. 75.
[48] P. J. Brown, K.-U. Neumann, and K. R. A. Ziebeck, J. Phys.: Condens. Matter **13**, 1563 (2001).
[49] F. J. Pinski, J. B. Staunton, and D. D. Johnson, Phys. Rev. B **57**, 15 177 (1998).
[50] V. L. Moruzzi, J. F. Janak, and K. Schwarz, Phys. Rev. B **37**, 790 (1988).
[51] J. Crangle and G. C. Hallam, Proc. R. Soc. London, Ser. A **272**, 119 (1963).
[52] G.-P. Renaud, Ph.D thesis, Lausanne University, 1988.
[53] G. Hausch and H. Warlimont, Acta Metall. **21**, 401 (1973).
[54] D. Bonnenberg, K. A. Hempel, and H. P. J. Wijn, in *Numerical Data and Functional Relationships in Science and Technology*, Landolt-Börnstein, New Series, Group III, Vol. 19, Pt. a (Springer, Berlin, 1986), p. 239.
[55] M. Podgorny, Phys. Rev. B **46**, 6293 (1992).
[56] G.-P. Renaud and S. G. Steinemann, J. Magn. Magn. Mater. **45**, 126 (1984).
[57] Ll. Mañosa, G. A. Saunders, H. Rahdi, U. Kawald, J. Pelzl, and H. Bach, J. Phys.: Condens. Matter **3**, 2273 (1991).
[58] Ll. Mañosa, G. A. Saunders, H. Rahdi, U. Kawald, J. Pelzl, and H. Bach, Phys. Rev. B **45**, 2224 (1992).
[59] M. M. Abd-Elmeguid and H. Micklitz, Physica B **161**, 17 (1989); Phys. Rev. B **40**, 7395 (1989).
[60] P. J. Brown, B. Roessli, J. G. Smith, K.-U. Neumann, and K. R. Ziebeck, J. Phys.: Condens. Matter **8**, 1527 (1996).